An Analysis of SeaWinds-Based Rain Retrieval in Severe Weather Events

Jeffrey R. Allen and David G. Long, *Senior Member, IEEE*

***Abstract*—The Ku-band SeaWinds scatterometer estimates near-surface ocean wind vectors by relating measured backscatter to a geophysical model function for the near-surface vector wind. The conventional wind retrieval algorithm does not explicitly account for SeaWinds' sensitivity to rain, resulting in rain-caused wind retrieval error. A new retrieval method, termed "simultaneous wind/rain retrieval," that estimates both wind and rain from rain-contaminated measurements has been previously proposed and validated with Tropical Rain Measuring Mission data. Here, the accuracy of rains retrieved by the new method is validated through comparison with the Next Generation Weather Radar (NEXRAD) in coastal storm events. The rains detected by both sensors are comparable, though SeaWinds-estimated rains exhibit greater variability. The performance of simultaneous wind/rain retrieval in flagging excessively rain-contaminated winds is discussed and compared to existing methods. A new rain-only retrieval algorithm for use in rain-backscatter-dominated areas is proposed and tested. A simple noise model for SeaWinds rain estimates is developed, and Monte Carlo simulation is employed to verify the model. The model shows that SeaWinds rain estimates have a standard deviation of 2.5 mm/h, which is higher than the NEXRAD measurements. Thresholding SeaWinds rain estimates at 2 mm/h yields a better rain flag than current rain flag algorithms.**

***Index Terms*—Next Generation Weather Radar (NEXRAD), QuikSCAT, rain, scatterometer, SeaWinds, simultaneous wind/rain retrieval, wind.**

I. Introduction

SCATTEROMETERS such as SeaWinds are designed to measure the near-surface wind speed and direction over the ocean's surface [1]. They do this indirectly by measuring the normalized radar cross section (σ°) and inverting a geophysical model function (GMF) relating the near-surface vector wind to σ° [2]. Unfortunately, the accuracy of SeaWinds wind estimates are often degraded in the presence of rain [3]–[5] which affects 4% to 10% of SeaWinds measurements [6]. Often, this degradation is manifested through a bias in the retrieved wind direction.

Conventional wind estimates are adversely affected because the retrieval algorithm does not explicitly account for the sensitivity of the backscatter measurements to rain. Recently, a new retrieval algorithm has been developed that exploits SeaWinds' sensitivity to rain to simultaneously retrieve the vector wind and the vertically integrated rain rate [7]. Validation of SeaWinds rain retrieval has been performed through Cramer–Rao bound analysis, Monte Carlo simulation, and comparison with Tropical Rain Measuring Mission (TRMM) Precipitation Radar [7] and TRMM Microwave Imager (TMI)-estimated rains [6].

In this paper, we validate SeaWinds simultaneous wind/rain (SWR) retrieval rain estimates by comparison with collocated rains observed by the WSR-88D Next Generation Weather Radar (NEXRAD) in severe storm events. We evaluate the accuracy of the instantaneous rains estimated by simultaneous wind/rain retrieval and conditions that affect that accuracy. After presenting background describing SWR retrieval and NEXRAD rain retrieval in Section II, we develop a comparison method in Section III. The application of SWR retrieval for rain flagging and wind quality assessment is analyzed in Section IV. A simple noise model is used in Section V to examine the variability of the SeaWinds rain observations. Conclusions are provided in Section VI.

II. Data

A. Simultaneous Wind/Rain Retrieval

In this paper, we utilize SeaWinds measurements provided by SeaWinds-on-QuikSCAT (1999–present) and SeaWinds-on-ADEOS-II (2003). These instruments report the normalized radar cross section (σ°) of the ocean's surface at a variety of azimuth angles using a rotating, dual-beam antenna. The inner beam is H-polarized and has an incidence angle of approximately 46° producing a 1400-km-wide inner swath, while the outer beam is V-polarized with a 54° incidence angle and covers a 1800-km-wide swath. For most of the inner swath, the instrument retrieves σ° measurements from at least four distinct azimuth angles [1].

SeaWinds σ° measurements are spatially gridded into 25 km $\times$ 25 km wind vector cells (WVCs). The center 18 WVCs are in the near-nadir region where the reduced measurement azimuth diversity degrades the wind retrieval accuracy. Measurements made in the so-called "sweet spot" in the off-nadir inner swath have greater azimuth diversity and correspondingly higher estimation skill [1], [8].

For each WVC, the near-surface wind vector is estimated by inverting the GMF given collocated σ° measurements using a maximum-likelihood (ML) estimator [2], [8]. Assuming Gaussian white noise and independent samples, the probability of the σ° measurements given near-surface wind velocity and direction $\vec{u}$ is

$$p(\vec{z}|\vec{u}) = \prod_k \frac{1}{\sqrt{2\pi}\zeta} \exp\left(-\frac{1}{2}\frac{(z_k - M(\vec{u},\phi_k))^2}{\zeta^2}\right) \quad (1)$$

Manuscript received March 3, 2005; revised August 22, 2005.

The authors are with the Department of Electrical and Computer Engineering, Brigham Young University, Provo, UT 84602 USA (e-mail: long@ee.byu.edu).

Digital Object Identifier 10.1109/TGRS.2005.858431

where $\vec{z}$ is a vector of σ° measurements, $M(\vec{u}, \phi_k)$ is the GMF, and ζ^2 is the measurement variance [7]. The GMF is a function of wind vector $\vec{u}$, the instrument azimuth angle ϕ_k, the polarization, and the incidence angle.

SeaWinds estimates the wind by taking the negative logarithm of (1), dropping constant terms and applying an iterative search routine to find a minima [9]. In the case of multiple solutions (called ambiguities), ambiguity selection is performed using thresholded nudging [10] and an iterative median filter [11].

To improve wind estimate performance in the presence of rain, Draper and Long developed a GMF that explicitly accounts for the effects of rain [5]. They modeled the rain perturbed radar backscatter as [5]

$$\sigma_m = (\sigma_w + \sigma_{\rm rs})\alpha_r + \sigma_{\rm rb} \tag{2}$$

where σ_m is the received backscatter, σ_w is the backscatter due to the near-surface wind stress, $\sigma_{\rm rs}$ is additional backscatter due rain perturbation of the surface, α_r is the two-way signal attenuation due to the attenuation from hydrometeors, and $\sigma_{\rm rb}$ is the effective backscatter from falling rain. This model can be written in a simplified form as [5]

$$\sigma_m = \sigma_w \alpha_r + \sigma_e \tag{3}$$

where α_r is the effective two-way signal attenuation due to the attenuation from hydrometeors, and $\sigma_e = \sigma_{\rm rs}\alpha_r + \sigma_{\rm rb}$ is the net effective rain backscatter, which is due to falling hydrometeors and rain surface effects, including attenuation [7], [12].

The new GMF (M_r) is expressed in [6] as

$$M_r(\vec{u}, \phi_k, R) = M(\vec{u}, \phi_k)\alpha_r(R) + \sigma_e(R) \tag{4}$$

where R is the rain rate in kilometer-millimeters per hour. In [5], $\alpha_r(R)$ and $\sigma_e(R)$ are quadratic functions of R estimated from collocated rain measurements from the TRMM, wind vector estimates from the National Centers for Environmental Prediction (NCEP), and SeaWinds σ° measurements.

SWR retrieval requires multiple azimuth measurements and high instrument skill and thus may only be performed in inner-beam region of the swath. This limits the SWR retrieval swath width to 1400 km but still allows daily rain observations of at least 80% of the Earth's ocean surface. Inversion of the rain GMF is performed using ML techniques. Like conventional retrieval, SWR can result in multiple solutions necessitating an ambiguity selection algorithm that considers rain [7].

The SeaWinds observations of wind and rain can be divided into three regimes [5]. In Regime 1, the observed σ° is dominated by rain. In Regime 2, wind and rain contributions to σ° are of the same order. In Regime 3, σ° is wind-dominated and rain has a negligible effect. The regions are defined through thresholding the estimated rain induced backscatter (σ_e°) and the measured backscatter (σ_m°). Regime 1 contains areas in which $\sigma_e^\circ/\sigma_m^\circ \geq 0.75$, and Regime 3 contains areas in which $\sigma_e^\circ/\sigma_m^\circ \leq 0.25$. Regime 2 is the intermediate region. The regimes help in understanding the conditions in which wind or rain information can be extracted. Wind data from Regime 1 and rain data in Regime 3 may be unobtainable. Simultaneous wind and rain estimates can be obtained for data in Regime 2.

In order to limit errors, the maximum retrieved rain rate is limited to 100 km·mm/h in the retrieval algorithm. To convert the SeaWinds rains from kilometer-millimeters per hour to millimeters per hour for comparison to NEXRAD observations, we must know the storm height. Lacking adequate information, for simplicity we scale SeaWinds rain by 1/8, corresponding to an 8-km maximum height of severe weather events. This value is used for all cases in this paper. The rain column height affects the relative calibration of the SeaWinds and NEXRAD rain rates, but does not affect the correlation coefficient used to compare them.

B. NEXRAD Rain Retrieval

In order to evaluate the accuracy of SeaWinds-based rains, we compare the SeaWinds-derived rain rate to collocated rain rate observations provided by coastal NEXRAD radar stations. Here, we discuss NEXRAD rain retrieval.

NEXRAD measures radar reflectivity and Doppler shift by employing a rotating 8.5-m paraboloid antenna [13], [14]. The 750-kW radar operates at S-band (2.7–3.0 GHz) and, while observing storm events, successively scans 360° in azimuth angle in 1° increments and from 0.5° to 16.5° in 1° increments in elevation angle. The radar also performs an additional circular scan at a 19.5° elevation angle. NEXRAD generally rotates at 3.4 rpm and completes a volume scan approximately every 5 min [13].

From reflected power measurements P_r collected by NEXRAD, estimates of reflectivity Z are computed using

$$Z = \frac{2^{10}(\ln 2)}{\pi^3 c}\frac{\lambda^2}{P_t \tau G^2 \theta_{3\,\rm dB}^2}\frac{r^2 P_r}{|K|^2} \tag{5}$$

where c is the speed of light in a vacuum, λ is the transmitted wavelength, P_t is the transmitted power, τ is the pulse duration in seconds, G is the antenna gain, $\theta_{3\,\rm dB}$ is the 3-dB antenna beamwidth, r is the range to target, and K is the complex index of refraction for water [13], [14]. Z is estimated at 1-km resolution over the range of 1–460 km from the radar.

In general, the reflectivity to rain rate (Z-R) relationship is modeled as

$$Z = {\rm a}R^{\rm b} \tag{6}$$

where a and b are storm-dependent (drop size distribution dependent) constants [15]. Through numerous aircraft observations Jorgensen and Willis determined the Z-R relationship of mature hurricanes to be $Z = 300R^{1.35}$ [16]. The rain rate for a given volume scan can be determined by inverting the Z-R relationship using Z values in NEXRAD Level II data provided by the NOAA Radar Operations Center.

The maximum range of the NEXRAD radar varies with storm orientation and intensity. In this study we limit our comparison to a subjectively determined, maximum useful range. For each of the events presented the maximum useful range varies between 200 and 350 km.

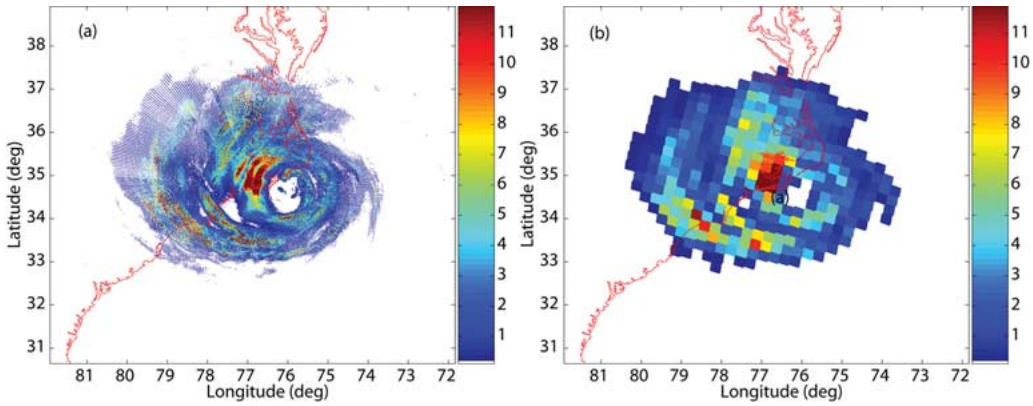

Fig. 1. Rain rate data from the Moorehead City, NC NEXRAD installation averaged into (a) 1 km × 1 km and (b) SeaWinds 25 km × 25 km WVC-sized vertical bins from Hurricane Isabel's landfall (September 18, 2003, 16:00 UTC) displayed on a latitude/longitude grid.

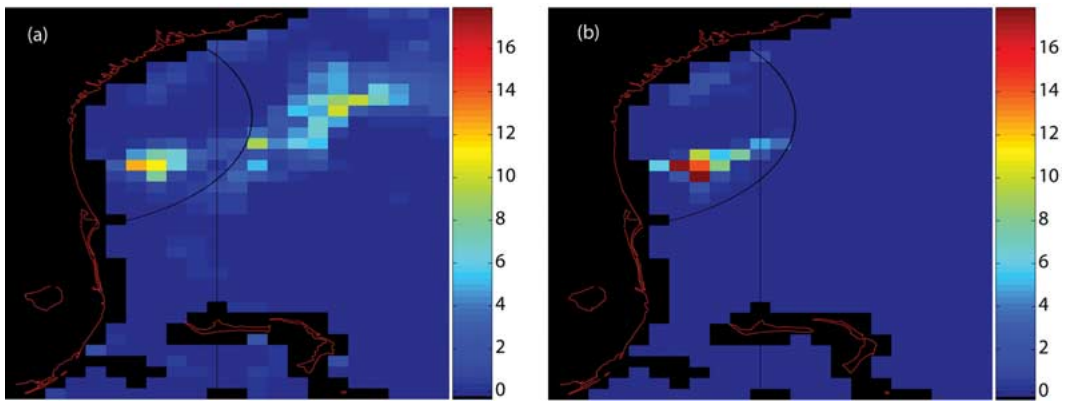

Fig. 2. (a) SeaWinds and (b) NEXRAD rain rates for a low wind/rain observation (August 27, 2004) in millimeters per hour. Black indicates areas in which SeaWinds did not retrieve wind or rain due to proximity to land. The axes are aligned with the along-track (vertical, which is roughly northward) and cross-track (horizontal) WVC grid. Each rectangular resolution element is 25 km × 25 km. The area to the left of the vertical line is in the nadir region of the SeaWinds swath, while the area to the right of the line is in the sweet spot. The circular line delineates NEXRAD's maximum useful range for this case.

III. Approach

Our goal in this paper is to compare SeaWinds-retrieved rainrate estimates with spatially and temporally collocated NEXRAD rainrate measurements under hurricane conditions. Winds are not considered in this paper for lack of a source of adequate high-resolution surface wind measurements.

Our comparison of SeaWinds and NEXRAD rains is made by evaluating collocated rain intensity data from each sensor. To ensure temporal collocation, only NEXRAD data observed within 5 min of the SeaWinds observation is considered. In order to compare SeaWinds and NEXRAD rains we need to account for the scales on which the sensors report rain.

SWR retrieval reports a single rain rate for each 25 km × 25 km WVC. This is treated as the vertically integrated and horizontally averaged rain rate over the WVC in this paper. Although the individual SeaWinds backscatter measurements are made at oblique angles, multiple backscatter measurements with different azimuth angles are combined to estimate the rain and these do not cover the same volume. For this reason, we ignore slant effects. At the SeaWinds incidence angles (46° and 54°), the horizontal displacement due to rain at altitude is approximately the same as the altitude. This displacement is relatively small compared to the 25 km × 25 km WVC and the antenna footprints, particularly since most rain occurs in the lower 4–5 km. Errors in the integration and averaging approximations tend to increase the variability in the NEXRAD/SeaWinds comparison.

NEXRAD rain is reported in 1-km range bins along each incidence and azimuth angle in the volume scan. In order to create rain values with comparable resolution to the SeaWinds values, the NEXRAD rain rate is spatially and vertically averaged over each 25 km × 25 km SeaWinds WVC. To determine the average NEXRAD rain rate for a given WVC, we average all the NEXRAD measurements that are located vertically above the WVC, subject to a maximum observation height of 10 km. We found that using the 10-km ceiling eliminates scattering from nonrain sources in the upper atmosphere while preserving rain information and correlation with SeaWinds-based rains. Averaging in this manner provides a compatible measurement of the rain on the same spatial scale reported by SeaWinds.

To illustrate our approach, Fig. 1 displays the NEXRAD rain that has been averaged into 1 km × 1 km vertical bins and the SeaWinds WVCs for Hurricane Isabel's landfall (September 19, 2003). To create Fig. 1(a), a 1 km × 1 km resolution grid is defined in the along-track/cross-track coordinate system of SeaWinds. Then, NEXRAD measurement locations as reported in the NEXRAD data files are located on this grid. Where multiple (including those at different heights) measurements fall into the same spatial grid element, they are averaged. The resulting average is then plotted at its corresponding latitude/longitude po-

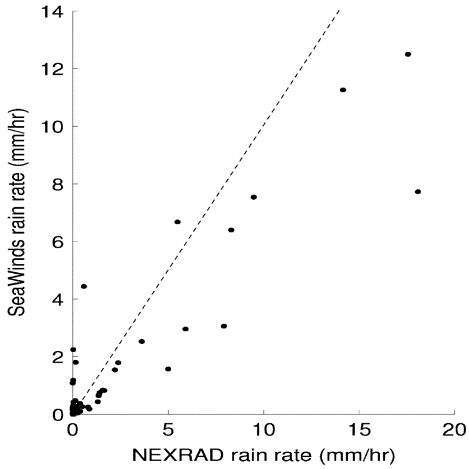

Fig. 3. Scatter plot of SeaWinds and NEXRAD integrated rain rates corresponding to Fig. 2. The data have a correlation coefficient of 0.92 and include all 85 ocean points that fall within the circle in Fig. 2. In this and later plots, $y = x$ is indicated by the dashed line.

sition. To create Fig. 1(b), the same process was used but with the 25 km $\times$ 25 km resolution SeaWinds WVC grid.

In the ideal case, rain rates retrieved by both sensors are linearly related by a constant. In this study the correlation coefficient is used as a metric to evaluate the relationship of the rain rates. Evaluation is also made by comparing rain maps from both sensors.

For baseline validation purposes, NEXRAD and SeaWinds rain data from an arbitrarily chosen nonhurricane event are analyzed. NEXRAD radar data from Jacksonville, FL on August 27, 2004 at 10:55 UTC is compared with collocated SeaWinds rain estimates in Fig. 2. NEXRAD's approximate maximum useful range (300 km) and key portions of the SeaWinds swath are indicated in the figure. Conventionally retrieved wind speeds from SeaWinds are within 5–26 m/s (mean 10.7 m/s) inside the NEXRAD coverage area.

Fig. 2 shows that SeaWinds and NEXRAD estimated rain rates have high spatial correlation. Both sensors detect the storm extending east from central Florida with similar rain rates. A scatter plot of the rain observed by both sensors is shown in Fig. 3. While the number of comparison points is small, in general, the rain rates from both sensors agree within 4 mm/h. The correlation coefficient of the rain rates is 0.9241, which demonstrates the high linear dependence of the rain rates. The mean observed rain rates are 1.3 and 1.0 mm/h for NEXRAD and SeaWinds, respectively.

In order to evaluate the behavior of SeaWinds rains at high rain rates and wind speeds we consider recent hurricane events. Five storm observations are considered: Hurricane Isabel's landfall (September 18, 2003, 16:00 UTC), Hurricane Alex's approach on the Florida coast (August 1, 2004 10:30 UTC), and three observations of Hurricane Frances' landfall (September 4, 2004 10:55 UTC, September 4, 2004 23:15 UTC, and September 5, 2004 10:30 UTC). The number of study cases is limited by available simultaneous SeaWinds and NEXRAD hurricane observations. Conventionally estimated wind speeds derived from SeaWinds data vary from 2.8–38 m/s for these cases within the NEXRAD overlapping coverage. Alex had the lowest wind speed range of 2.8–25 m/s with a mean wind speed of 11 m/s while the first Frances case had the highest speeds (8.7–38 m/s with a mean of 20 m/s).

To illustrate the behavior of SeaWinds-based rain retrieval in severe storms, in Fig. 4 we present instantaneously collocated rain maps of Hurricane Isabel observed by NEXRAD in Morehead City, NC and by SeaWinds. We note that the rain maps from the two sensors are similar for the overlapping coverage areas. Each shows the hurricane eye just off the coast and strong rain bands to the south of the storm. Fig. 5 displays the corresponding scatter plot of the rain rates. We note that, although each instrument observes approximately the same rain rate in the mean, the variance in the comparison is relatively large. Compared to the previous analysis with lower winds and rains, in the higher wind speed and rain rates typical of hurricanes, the rain rate correlation of NEXRAD with SeaWinds is lower -0.68 versus 0.92.

Our study of the other four hurricane observations yields similar results to those of Hurricane Isabel, though with slightly better average correlation: the Hurricane eye and outer rain bands are easily observable and collocated in the rain maps. The correlation coefficient of SeaWinds and NEXRAD rains for individual cases falls between 0.82 and 0.71. The correlation coefficient of SeaWinds/NEXRAD comparisons from all five events is 0.75.

IV. SWR Retrieval-Based Wind Quality Assessment

As part of the SWR retrieval algorithm, the measurement regime can be inferred. This can be used as a wind quality assessment tool [7]. Additionally, the rain rate estimated by SWR retrieval can be used to augment existing rain flags. These applications are considered in the following.

A. Rain Flagging

In the Jet Propulsion Laboratory's L2B product, rain contamination in WVCs is flagged by the multidimensional histogram (MUDH) algorithm [9], [17]. This algorithm estimates the probability that a WVC is rain contaminated based on empirical analysis of the likelihood value, rain, and backscatter values. The probabilities provided by the algorithm are used to flag rain-contaminated WVCs when the rain rate exceeds approximately 2 mm/h.

Rain information provided by SWR retrieval can be converted to a rain flag algorithm by thresholding the rain rate. In this study, the rain threshold is set at 2 mm/h. A WVC is considered to be raining if the NEXRAD-determined rain rate exceeds 2 mm/h.

Two performance metrics are considered. The first is the "false alarm percentage," which is computed by determining the number of WVCs in which SeaWinds detects a rain rate greater than the threshold and NEXRAD detects no rain, divided by the total number of WVCs in which NEXRAD detects no rain and expressed as a percentage. The second metric is the "missed rain percentage," which is the number of WVCs in which the NEXRAD rain rate is greater than the threshold and SeaWind's rain rate is less than the threshold, divided by the number of WVCs in which the NEXRAD detects rain and expressed as a

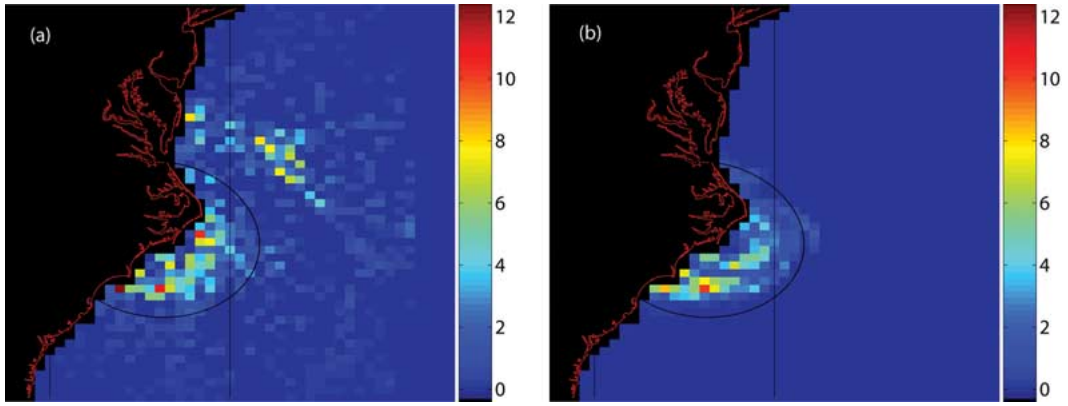

Fig. 4. (a) SeaWinds and (b) NEXRAD rain rates for Hurricane Isabel's landfall (September 18, 2003, 16:00 UTC). Black indicates areas in which SeaWinds did not retrieve rain. See caption of Fig. 2 for explanation of circle and line.

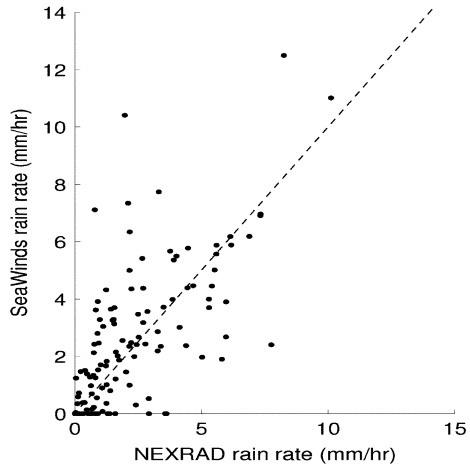

Fig. 5. SeaWinds and NEXRAD (124 points) rain rate scatter plots for Hurricane Isabel landfall. The correlation coefficient is 0.68.

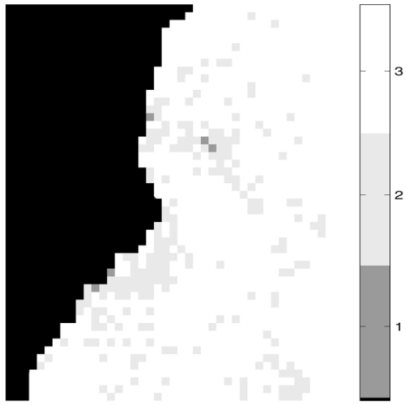

Fig. 6. SeaWinds-classified regimes for SeaWinds' observation of Hurricane Isabel. Regime 1 is rain-dominated. Regime 3 is wind-dominated, and Regime 2 is the intermediate case where the observed radar backscatter is similarly affected by wind and rain. Black denotes land.

percentage. Over all the hurricane events studied in this paper, the false alarm percentage for the SWR rain retrieval is 0.21% and the missed rain percentage is 23%.

For comparison, we compute the SeaWinds MUDH rain flag performance [17]. To ensure consistency, a MUDH rain flag threshold is determined by finding a threshold value which results in flagging the same percentage of WVCs as the 2 mm/h NEXRAD threshold. For the hurricane cases, the corresponding MUDH threshold is 90%, which results in a MUDH false alarm percentage of 0.62% and a missed rain percentage of 26% for the regions studied. The MUDH metrics are larger than corresponding SWR rain flag percentages, and we conclude that the SWR algorithm provides an improved rain flag, particularly for false alarms. False alarm performance is important since rain occurs in only 4% to 10% of SeaWinds WVCs.

B. Wind/Rain Regimes

Here we analyze SWR rain performance based on the regimes discussed in Section II. It is expected that rain rates may be estimated for WVCs in Regimes 1 and 2, but not in Regime 3 where the rain has little impact on the observed backscatter [7]. We note that wind estimation is not affected by rain in Regime 3, is somewhat affected by rain in Regime 2, and should not be used in the rain-dominated Regime 1. Thus, identification of the wind/rain regime provides a quality flag on the estimated wind and rain.

To illustrate regime classification, Fig. 6 displays a map of the SWR-classified regimes for SeaWinds' observation of Hurricane Isabel. Most WVCs near the eye of the hurricane and in the outer rain bands are classified in Regime 2. The eye and points distant from the hurricane are classified in Regime 3. A few WVCs in the northern and southern rain bands are classified in Regime 1. Although no independent validation of this classification is available, the pattern of classification in this map is considered reasonable since there is generally little rain inside the eye, high wind speeds and rain rates are common on the eye-wall, and high rain rates with decreasing wind speeds typically occur in the outer rain bands.

Scatter plots of rain rates observed by NEXRAD and SeaWinds for all cases considered in this paper are shown by regime in Fig. 7. Most WVCs with high SeaWinds and NEXRAD rain rates are in Regime 1. WVCs with low SeaWinds and NEXRAD rain rates are in Regime 3. Regime 2 contains a mix of relatively high and low rain rates. The correlation coefficients between SWR and NEXRAD from rates for the first, second, and third regimes are 0.59, 0.61, and 0.40, respectively. Low correlation

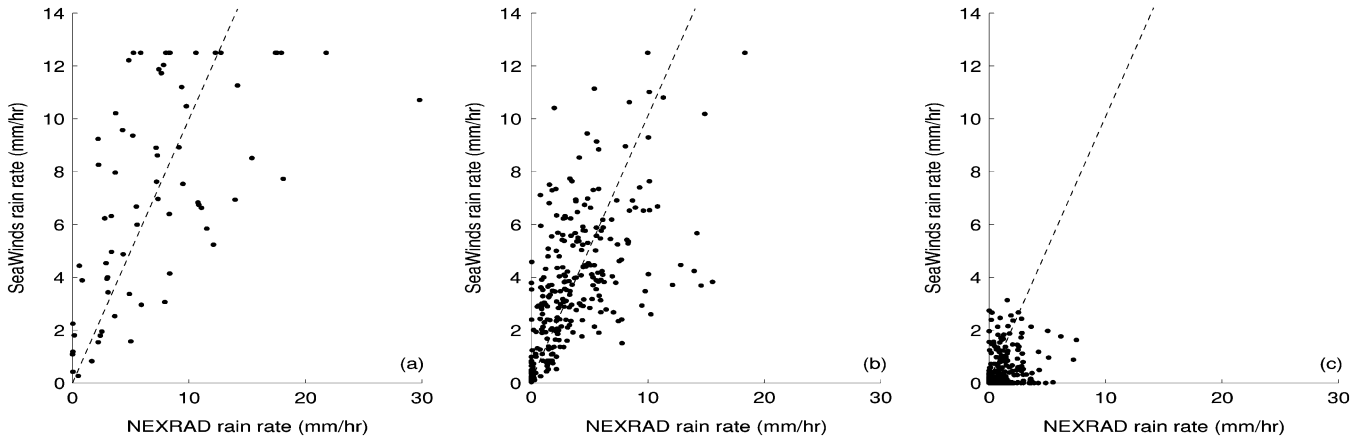

Fig. 7. Scatter plot of NEXRAD versus SeaWinds rain rates for (a) Regime 1 (70 points), (b) Regime 2 (283 points), and (c) Regime 3 (479 points). The correlation coefficient for each regime is 0.59, 0.62, and 0.40, respectively.

in Regime 3 is expected because σ° in the regime is wind-dominated and rain rate estimation is poor.

We note that the correlation coefficient of each regime is less than the correlation coefficient of the combined dataset (0.72). This is due to the separation of the data in Regime 3 from the other regimes. Regime 3 rain rates are smaller than rates from the other regimes, reducing the variance and increasing the correlation coefficient of the combined set.

Although rain-dominated, rain estimates in Regime 1 do not exhibit improved correlation over Regime 2 rain. This may be due to interference from σ° induced by wind, though the fixed storm height calibration factor could be playing a role. We also note that SWR is used to estimate both wind and rain for all regimes. However, in Regime 1 the observed σ° is expected to be rain dominated, suppressing wind information. SWRs attempt to retrieve wind in Regime 1 may add variability to the rain estimates as the wind becomes a nuisance parameter. Regime 1 rain estimates may be improved by performing rain-only retrieval.

A simple rain-only retrieval algorithm is developed by forming a rain-only GMF (M_{rain})

$$M_{\text{rain}} = \sigma_e(R) \tag{7}$$

where $\sigma_e(R)$ is a quadratic function of R as described in [5]. Given backscatter measurements, the rain rate is determined by finding the least squared error $e(R_{\text{dB}})$ between the measurements and the model function

$$e(R_{\text{dB}}) = \sum_{i=1}^{n} (\hat{\sigma}_i - \sigma_{ei}(R_{\text{dB}}))^2 \tag{8}$$

where R_{dB} is the rain rate in decibels normalized to 1 mm/h, $e(R_{\text{dB}})$ is the error function, $\hat{\sigma}_i$ is the SeaWinds ith σ° measurement for the WVC of interest, and $\sigma_{ei}(R_{\text{dB}})$ is the GMF for the ith measurement and n is the number of σ° measurements in the WVC. The error function is minimized by taking the derivative of (8), setting it to zero, dropping constant terms, and solving for the rain rate. Since σ_{ei} is a quadratic function, the derivative of (8) is cubic and the estimated R_{dB} is set to the smallest real root.

For accurate rain-only retrieval, the wind contribution to σ° must be negligible. Areas where wind-only retrieval are performed are restricted to the rain-dominated Regime 1, as identified by the SWR retrieval algorithm. Fig. 8 displays SeaWinds and NEXRAD rain rate estimates for SWR and rain-only retrieval for the nonhurricane case. In Regime 1, the correlation coefficient of the SWR and NEXRAD collocated rains is slightly improved from 0.88 to 0.89 and the variance of the rain estimates decreases.

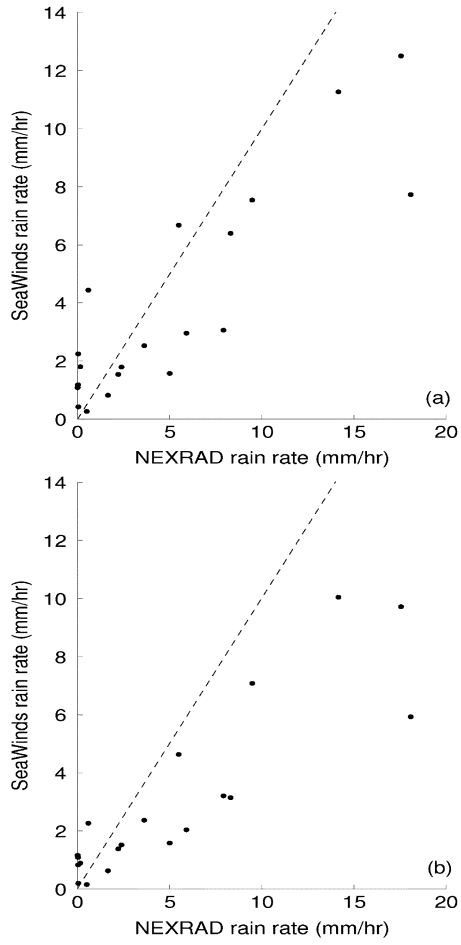

Fig. 8. Scatter plot of NEXRAD versus SeaWinds rains for simultaneous (a) wind/rain and (b) rain-only retrieval in Regime 1 WVCs from the nonhurricane case (August 27, 2004). Use of rain-only retrieval increases the correlation coefficient from 0.88 in (a) to 0.89 in (b). Both datasets consist of 20 points.

Correlation of Regime 1 data from Hurricane Alex is increased through the use of rain-only retrieval; however, in the other Hurricane events, which have larger winds, correlation with NEXRAD rains decreases when rain-only retrieval is performed. We speculate that this is most likely due to higher wind speeds and misclassification of the data regime.

V. Noise Modeling and Simulation

Rain retrieval is a serendipitous application of the SeaWinds data which was originally designed only for wind measurement. To provide an approximate model for the random component of the rain estimate error, in this section we identify the noise sources in the rain retrieval process, and introduce a simple noise model. The noise model is then employed to simulate the error in SWR rain retrieval and infer the accuracy and principal noise sources of SeaWinds-based rain measurements. The model is developed in terms of rain rate.

A primary source of variability in NEXRAD rain estimates is due to noisy Z detection resulting from noisy P_r measurements. P_r is computed from the returned signal envelope through a combination of time and range averaging. Averaging is performed to reduce the standard deviation (σ) of the Z estimate to 1 dB [13], [14]. Fig. 9(a) displays hurricane rain rate versus $\mathrm{Z} \pm \sigma$. The difference between the σ envelope edges increases with rain rate. Fig. 9(b) displays the σ difference between the zero noise rain rate and the rain rate when the Z estimate differs from the true Z by $\pm\sigma$. NEXRAD's rain rate estimation σ in hurricane events for rain rates greater than 2 mm/h is approximately $0.2R$. In absence of other factors, the NEXRAD rain rate (R_N) observation model is related to the true rain rate (R_t) by

$$R_{\mathrm{NEXRAD}} = |R_t(1 + \alpha_1\nu_1)| \tag{9}$$

where $\alpha_1 = 0.2$ and ν_1 is a zero mean, unit variance, Gaussian random variable. Due to the large number of independent scatterers and Z estimation error sources, the central limit theorem suggests that ν_1 can be assumed to be Gaussian. The absolute value operator ensures that the reported rain is nonnegative.

SeaWinds rain estimation variability is caused primarily by three sources: "communication error," beamfilling, and imperfect collocation of the backscatter measurements for a given WVC. Communication error variability in the σ° measurements is due primarily to radiometric emissions and thermal noise [8].

SeaWinds does not uniformly sample each WVC. The beam has a nonuniform antenna beam pattern that integrates backscatter over its footprint [5]. Rain has high spatial variability and is rarely uniform over a given WVC, resulting in an effect known as nonuniform beam-filling. Further, due to the variability of the rain over the WVC and the fact that the various measurement footprints do not precisely overlap and align, the different SeaWinds observations may "see" different rain rates. This imperfect collocation effect increases the variability of SeaWinds rain estimates [7].

This study compares NEXRAD and SeaWinds observations that are collocated by the spatial extent of the SeaWinds WVC at the surface. As previously noted, due to their observation geometries, the observations are not necessarily collocated at higher altitudes (see the discussion in [5]). This vertical misregistration also increases the variability in the rain rate comparisons.

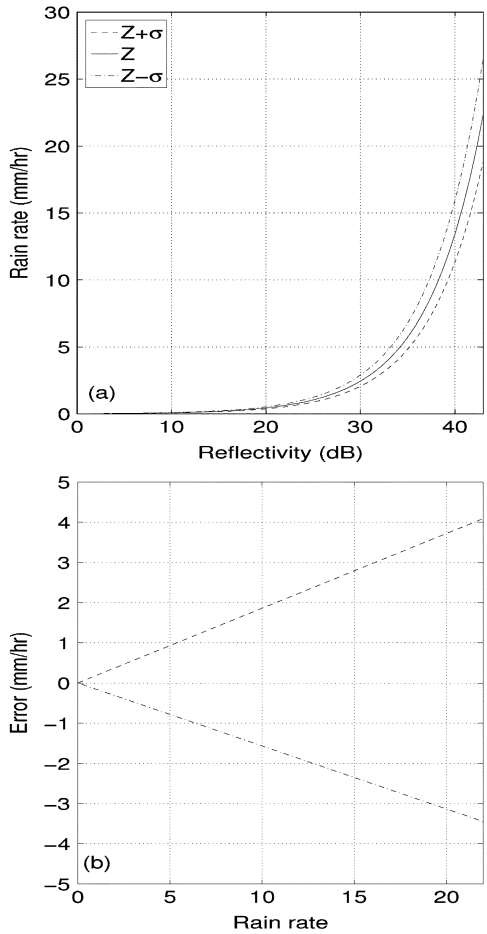

Fig. 9. (a) NEXRAD rain rate versus reflectivity. Rain rate is plotted as a function of Z with $\pm\sigma$ envelopes. The solid line is the nominal Z-R relationship, and the dotted lines show the relationship when $\mathrm{Z} = \mathrm{Z} \pm \sigma$ where $\sigma = 1$ dB. (b) Differences between calculated and true rain rate for $\mathrm{Z} \pm \sigma$. The standard deviation of the rain rate estimation is approximately 0.2 R, where R is the true rain rate.

A simple noise model may be employed to investigate the variability of SeaWinds-based and NEXRAD rain rates. This model ignores the wind. We note that although the variability due to NEXRAD Z detection is multiplicative, the variability of the scatter plots in Section IV appears to be primarily driven by additive error. The multiple uncorrelated sources of SeaWinds rain variability suggest that for a simple model, R_S can be expressed as

$$R_S = |R_t + \alpha_2\nu_2| \tag{10}$$

where α_2 is constant and ν_2 is a unit variance zero mean Gaussian random variable. Combining (9) and (10) yields

$$R_S = |R_N(1 + \alpha_1\nu_1) + \alpha_2\nu_2| \tag{11}$$

where ν_1 and ν_2 are uncorrelated Gaussian random variables with zero mean and unit variance α_1 and α_2 are the standard deviations of the additive SeaWinds and NEXRAD estimation errors.

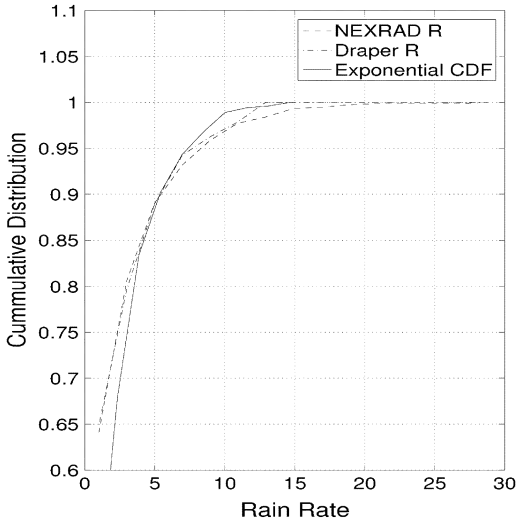

Fig. 10. Cumulative distribution functions of the NEXRAD and SWR rain rates for all hurricane events and an exponential distribution with the same mean and variance as the NEXRAD rain rates.

A. Simulation

Monte Carlo simulation is employed to estimate α_2, the additive component in the noise model. We may then infer the variability of SeaWinds-based rains. For the Monte Carlo simulation, the distribution of R_t is needed. Fig. 10 displays the cumulative density functions (CDFs) of the NEXRAD and the SeaWinds SWR rain rates for all cases studied, along with a scaled exponential CDF with the same mean and variance as the observed NEXRAD rain rates. While the exponential and NEXRAD CDFs exhibit differences in low rain rates, the CDFs exhibit enough similarity that it is reasonable to model the distribution of Hurricane rain as exponential with the mean and variance of the NEXRAD rain rate in this simple first-order simulation.

Monte Carlo simulation is performed by creating 1000 exponentially distributed realizations of R_t for each of several values of α_2. Then, for each realization of R_t, a R_N realization is produced through (9). Next, using (10), realizations of R_S are created. Finally, the correlation coefficient of the R_N and R_S realizations is determined for each value of α_2.

The results of the Monte Carlo simulation are displayed in Fig. 11 as a plot of α_2 versus the correlation coefficient. The correlation coefficient nears 0.75 (the approximate correlation of the actual NEXRAD and SeaWinds rain correlations) when $\alpha_2 \approx 2.5$ mm/h. For illustration, a scatter plot of the first 100 simulated NEXRAD and SeaWinds rain estimates for the simulation with $\alpha_2 = 2.5$ is displayed in Fig. 11. The scatter plot is similar to the scatter plots found for the hurricane events.

Our simulation thus suggests that we may treat the total noise on SeaWinds rain estimations as a zero mean Gaussian random variable with a standard deviation of 2.5. Draper and Long [6] estimated that SeaWinds rain retrieval is generally within 3 dB of the true rain. Monte Carlo simulation for Hurricane rains shows that the standard deviation of the SeaWinds rain estimate is within 3 dB of the true rain for all rates greater than 6 mm/h, which confirms the error estimate of [6].

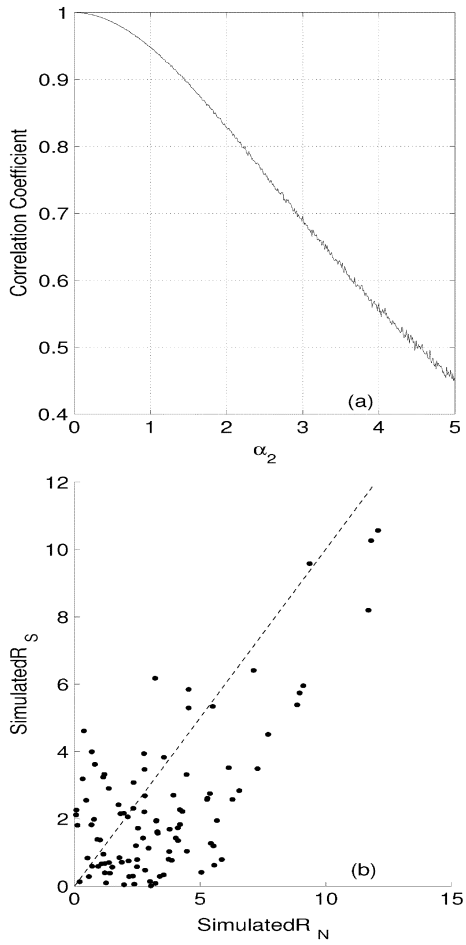

Fig. 11. Monte Carlo simulation result for the simple SeaWinds/NEXRAD noise model. (a) Shows α_2 versus correlation coefficient for the additive noise Monte Carlo simulation. Correlation nears 0.75 when α_2 is 2.5. (b) Displays the scatter plot created simulation at $\alpha_2 = 2.5$.

VI. Conclusion

The SeaWinds scatterometer was originally designed to measure near-surface ocean winds. However, simultaneous wind/rain retrieval enables the instrument to simultaneously estimate both wind and rain—at least under most conditions. Prior validation studies compared SeaWinds-derived rain with TRMM PR and TRMM TMI. Here, we compared SeaWinds-derived rain with NEXRAD. The results show that SeaWinds-derived rain rates, though noisy, provide useful rain information. SeaWinds rain estimates degrade somewhat in high wind/rain events. However, even in such events the estimated rain rate can yield a better rain flag than the current algorithm. The rain estimation performance is dependent on the wind/rain regime.

The simple noise model presented in this report produces simulated rains with statistics similar to those retrieved by SeaWinds and NEXRAD. The simulation illustrates that the variability in SeaWinds-based rain estimates may be modeled as the true rain rate with an additive noise source having a standard deviation of 2.5 mm/h.

ACKNOWLEDGMENT

SeaWinds and QuikSCAT data were obtained from the Physical Oceanography Distributed Data Archive (PO.DAAC) at the Jet Propulsion Laboratory, Pasadena, CA. NEXRAD data were obtained from the National Climatic Data Center. This work was completed at the Brigham Young University Microwave Earth Remote Sensing Laboratory.

REFERENCES

[1] D. Spencer, C. Wu, and D. Long, "Tradeoffs in the design of a spacebourne scanning pencil beam scatterometer: Application to SeaWinds," *IEEE Trans. Geosci. Remote Sens.*, vol. 35, no. 1, pp. 116–126, Jan. 1997.

[2] F. Naderi, M. Freilich, and D. Long, "Spaceborne radar measurement of wind velocity over the ocean-an overview of the NSCAT scatterometer system," *Proc. IEEE*, vol. 76, no. 6, pp. 850–866, Jun. 1979.

[3] R. Contreras, W. Plant, W. Keller, K. Hayes, and J. Nystuen, "Effects of rain on Ku-band backscatter from the ocean," *J. Geophys. Res.*, vol. 108, no. C5, pp. (34)1–(34)15, 2003.

[4] D. Weissman, M. Bourassa, and J. Tongue, "Effects of rain rate and wind magnitude on SeaWinds scatterometer wind speed errors," *Atmos. Ocean. Technol.*, vol. 19, no. 5, pp. 738–746, May 2002.

[5] D. Draper and D. Long, "Evaluating the effect of rain on SeaWinds scatterometer measurements," *J. Geophys. Res.*, 2004. DOI:10.1029/2002/JC001741.

[6] ——, "Assessing the quality of SeaWinds rain measurements," *IEEE Trans. Geosci. Remote Sens.*, vol. 42, no. 7, pp. 1424–1432, Jul. 2004.

[7] ——, "Simultaneous wind and rain retrieval using SeaWinds data," *IEEE Trans. Geosci Remote Sens.*, vol. 42, no. 7, pp. 1411–1423, Jul. 2004.

[8] T. Oliphant and D. Long, "Accuracy of scatterometer derived winds using the Cramer–Rao bound," *IEEE Trans. Geosci. Remote Sens.*, vol. 37, no. 5, pp. 2642–2652, Nov. 1999.

[9] Jet Propulsion Lab., "QuikSCAT science data product user's manual," California Inst. Technol., Pasadena, Rep. D-18053, 2003.

[10] B. Stiles, B. Pollard, and R. Dunbar, "Direction interval retrival with thresholded nudging: A method for improving the accuracy of QuikSCAT winds," *IEEE Trans. Geosci. Remote Sens.*, vol. 40, no. 1, pp. 79–89, 2002.

[11] S. Shaffer, R. Dunbar, S. Hsiao, and D. Long, "A median-filter-based ambiguity removal algorithm for NSCAT," *IEEE Trans. Geosci. Remote Sens.*, vol. 40, pp. 1973–1983, 9 2002.

[12] B. Stiles and S. Yueh, "Impact of rain of spaceborne Ku-band wind scatterometer data," *IEEE Trans. Geosci. Remote Sens.*, vol. 40, no. 9, pp. 1973–1983, Sep. 2002.

[13] Federal Cordinator for Meteorological Services and Supporting Research, "Doppler radar meteorological observations, Part B: Doppler radar theory and meteorology," NOAA, Boulder, CO, FCM-H11B-1990, Jun. 1990.

[14] ——, "Doppler radar meteorological observations, Part C: WSR-88D products and algorithms," NOAA, Boulder, CO, FCM-H11C-1991, Feb. 1991.

[15] J. Marshall and W. Palmer, "The distribution of raindrops with size," *J. Appl. Meteorol.*, vol. 5, pp. 165–166, 1948.

[16] D. Jorgensen and P. Willis, "A Z-R relationship for mature hurricanes," *J. Appl. Meteorol.*, vol. 21, pp. 356–366, 1982.

[17] J. Huddleston and B. Stiles, "A multidimensional histogram rain-flagging technique for SeaWinds on QuikSCAT," in *Proc. IGARSS*, vol. 3, 2000, pp. 1238–1240.

Jeffrey R. Allen received the M.S. degree in electrical engineering from Brigham Young University (BYU), Provo, UT, in 2005.

At BYU, he worked with the BYU Center for Remote Sensing, focusing on scatterometer applications of microwave remote sensing. He is currently working as a Systems Engineer for Raytheon Missile Systems, Tucson, AZ.

Mr. Allen is a member of Tau Beta Pi.

David G. Long (S'80–SM'98) received the Ph.D. degree in electrical engineering from the University of Southern California, Los Angeles, in 1989.

From 1983 to 1990, he was with the National Aeronautics and Space Administration (NASA) Jet Propulsion Laboratory (JPL), Pasadena, CA, where he developed advanced radar remote sensing systems. While at JPL, he was the Senior Project Engineer on the NASA Scatterometer (NSCAT) project, which was flown aboard the Japanese Advanced Earth Observing System (ADEOS) from 1996 to 1997. He was also the Experiment Manager and Project Engineer for the SCANSCAT scatterometer (now known as SeaWinds). In 1990, he joined the Department of Electrical and Computer Engineering, Brigham Young University (BYU), Provo, UT, where he currently teaches upper division and graduate courses in communications, microwave remote sensing, radar, and signal processing, is the Director of BYU's Center for Remote Sensing, and is the Head of the Microwave Earth Remote Sensing Laboratory. He is the Principal Investigator on several NASA-sponsored interdisciplinary research projects in microwave remote sensing and innovative radar systems. He has numerous publications in signal processing and radar scatterometry. His research interests include microwave remote sensing, radar, polar ice, signal processing, estimation theory, and mesoscale atmospheric dynamics. He has over 250 publications in the open literature.

Dr. Long has received the NASA Certificate of Recognition several times. He is an Associate Editor for the IEEE GEOSCIENCE AND REMOTE SENSING LETTERS.